Journal of Materials Chemistry A

Accepted Manuscript

This article can be cited before page numbers have been issued, to do this please use: F. Zhao, G. Zhao, X. Liu, C. Ge, J. Wang, B. Li, Q. Wang, W. Li and Q. Chen, *J. Mater. Chem. A*, 2014, DOI: 10.1039/C4TA00847B.

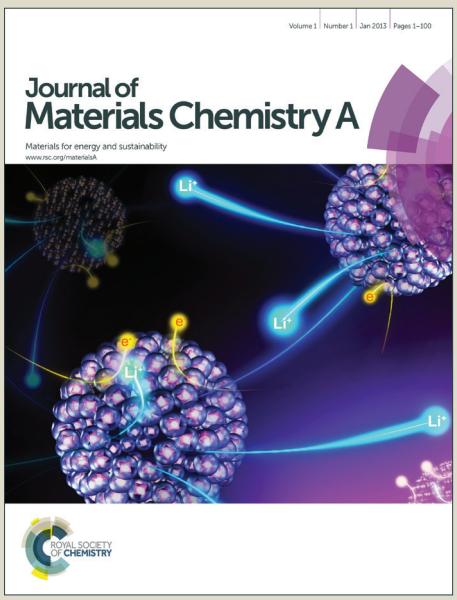

ROYAL SOCIETY OF CHEMISTRY

www.rsc.org/materialsA

View Article Online
DOI: 10.1039/C4TA00847B

Table of Contents

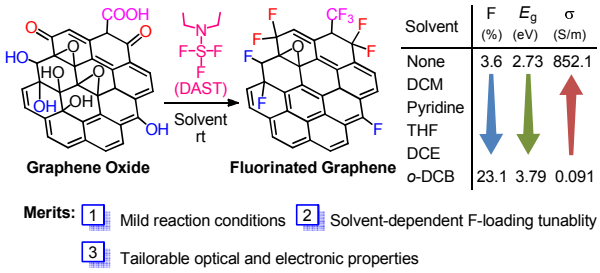

Fluorinated graphene with tuneable F-loading amount and properties was achieved via a facile solution approach using graphene oxide and liquid diethylaminosulfur trifluoride (DAST) as starting materials under mild conditions.

View Article Online
DOI: 10.1039/C4TA00847B

Journal Name

RSCPublishing

ARTICLE

Fluorinated graphene: facile solution preparation and tailorable properties by fluorine-content tuning†

Cite this: DOI: 10.1039/x0xx00000x

Received 00th January 2012,
Accepted 00th January 2012

DOI: 10.1039/x0xx00000x

www.rsc.org/

Fu-Gang Zhao,[a,‡] Gang Zhao,[b,‡] Xin-Hua Liu,[c] Cong-Wu Ge,[a] Jin-Tu Wang,[a] Bai-Li Li,[a] Qi-Gang Wang,*[c] Wei-Shi Li,*[a] and Qing-Yun Chen*[b]

Fluorinated graphene is one of the most important two-dimensional carbon nanomaterials derived from graphene, and possesses specific and outstanding properties. However, it lacks a cost-effective and massive preparation method. Here, we describe a novel and facile solution approach using graphene oxide (GO) and liquid diethylaminosulfurtrifluoride as starting materials under mild conditions. The chemical composition and the structure of so-prepared fluorinated graphene were characterized in detail by elemental analysis, solid state ^{19}F NMR, XPS, FT-IR, Raman, SEM, TEM, and AFM. These studies reveal that some oxygen-containing moieties in GO are converted into C–F bonds, while some are eliminated during the reaction. More interestingly, the fluorine-loading amount can be well tuned just by simply altering the reaction medium, and has significant impact on the optical, electronic, and conductive properties of the product. Preliminary experiments on their application as electrode materials for solid-state supercapacitors were finally presented.

Introduction

Fluorinated graphene (FG), in which fluorine atoms are covalently functionalized on carbon nanosheet skeletons, is a new type of two-dimensional carbon material.[1] Due to the unique nature of covalent F units, such as strong electronegativity and superhydrophobicity, fluorinated graphene possesses different properties from graphene. Perfluorinated graphene with one fluorine per carbon performs as a high quality insulating material with resistance larger than 10^{12} Ω, as well as with high thermal stability and mechanical strength.[2] Partially fluorinated graphene materials are semiconductors, whose bandgap is highly dependent on the fluorination extent.[3] Consequently, fluorination is a valid and facile way to open and tune the bandgap of graphene materials for their promising applications in electronics and photonics. Moreover, fluorinated graphene materials have been demonstrated in biomedical applications, such as promoting neuro-induction of stem cells,[4] and serving as a single multimodal material for magnetic resonance, ultrasound and photoacoustic imaging.[5]

The remarkable properties and promising applications of fluorinated graphene materials have motivated scientists to explore an effective method for their preparation. In pioneering works, exfoliation approach was adopted using graphite fluoride as starting materials, similar to that for graphene preparation from graphite.[2, 6] However, this method suffers from extremely low yield and the difficulty in fluorine-loading tuning. One alternative way is the fluorination of graphene nanosheets with gaseous agents, such as XeF_2,[7] F_2,[8] SF_6,[9] or CF_4,[10] without or with plasma assistance. Unfortunately, the most gaseous fluorination agents are expensive, highly toxic, hard to control and danger for large scale manipulation. Although fluoropolymers were reported as solid fluorination agents with the aid of laser irradiation, the work only demonstrated the selected area fluorination.[11] Obviously, these methods are far from desirable for cost-effective and massive production of fluorinated graphene materials.

As a cousin of graphene family, graphene oxide (GO) is densely decorated with hydroxyl, epoxy, carbonyl, and carboxyl functionalities on the surface and the edges of the sheet, and thus provides a variety of opportunities for chemical modification and transformation.[12] More importantly, GO can be conveniently and massively prepared from natural graphite in low cost. Recently, we envisioned that GO would be a promising starting material for cost-effective and massive preparation of fluorinated graphene if the oxygen-containing functionalities can be effectively transformed into C–F bonds. Along this line, we finally found diethylaminosulfurtrifluoride (DAST), a commercially available liquid fluorinating agent, is

ARTICLE View Article Online DOI: 10.1039/C4TA00847B Journal Name

efficient for such chemical transformations and thus convert GO to FG under mild conditions (Scheme 1). Of interest, the fluorine loading can be easily tuned just by simply changing the reaction medium. During our work, hydrofluoric acid and F_2 gas were successively reported to be also effective in such conversions.[13, 14] However, the method based on hydrofluoric acid was carried out under hydrothermal conditions, that require special apparatuses and high temperature (180 °C).[13] The use of F_2 gas would face with the similar hazardous issue as the previous works.[7–10]

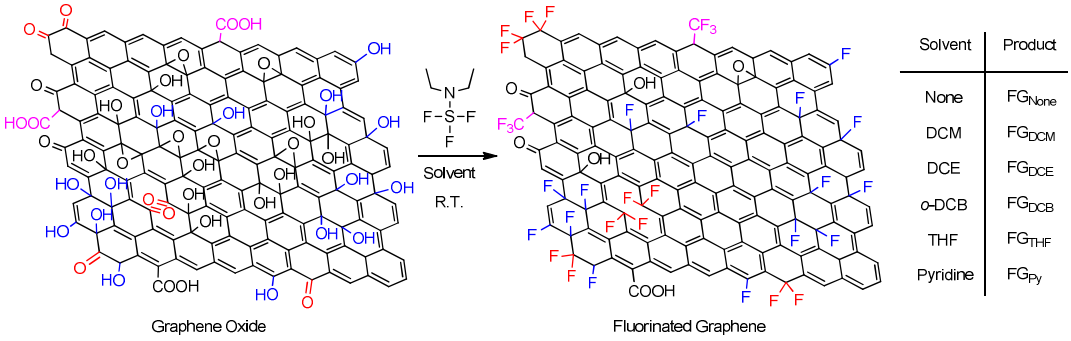

Scheme1 Schematic diagram for the synthesis of fluorinated graphene via the reaction between GO and DAST at room temperature.

Results and discussion

The conversion of GO[15] into FG with DAST was carried out in a PTFE flask. The suspension of GO (0.150 g in 150 mL solvent) was dropwise added with DAST (2.5 mL) at 0 ºC within 10 min, followed by sonication for 6 h and then stirring for 3 d at room temperature. After the reaction was carefully quenched with MeOH, the fluorinated graphene product was separated by filtration and subjected to thorough wash with ethanol, acetone, chloroform, tetrahydrofuran (THF) and deionized water. We found the reaction medium has great impact on the fluorination and the final products. Thus, we assigned the name of FG_{None}, FG_{DCM}, FG_{THF}, FG_{Py}, FG_{DCE}, and FG_{DCB} for the products obtained without solvent and in dichloromethane (DCM), THF, pyridine (Py), 1,2-dichloroethane (DCE) and *o*-dichlorobenzene (DCB), respectively.

Table 1 Elemental analysis data of GO and the fluorinated graphene products

Sample	F (%)	C (%)	H (%)	N (%)	O [a] (%)
GO	–	51.1	3.4	1.2	43.9
FG_{None}	3.6	62.8	3.1	1.1	29.4
FG_{DCM}	6.0	64.3	2.1	0.9	26.7
FG_{Py}	8.7	58.8	2.8	1.4	28.3
FG_{THF}	16.2	65.6	3.2	1.0	14.1
FG_{DCE}	17.5	64.5	2.4	0.7	14.9
FG_{DCB}	23.1	59.8	1.7	0.6	14.7

[a] O% = 100% - F% - C% - H% - N%

Table 1 lists the elemental analysis of all fluorinated products together with the raw material GO. From the data, it is clear that the fluorine-loading amount is highly dependent on the reaction medium. When GO was treated with DAST in solvent-free conditions, the product (FG_{None}) contained only 3.6% fluorine amount. However, if the reaction was carried out in THF, the fluorine loading of the product (FG_{THF}) dramatically increased to 16.2%. The fluorine contents can be further raised up to 17.5% and 23.1% with DCE and DCB as solvent, respectively. Furthermore, the increment in the carbon content for all fluorinated graphene products in comparison with GO was observed. However, if one considers that some oxygen-containing units in GO are transformed to fluorinated ones but the others remain intact, the carbon content should decrease owing to the larger atomic weight of F than that of O. The observed contrary result indicates GO nanosheets were simultaneously partially reduced during the fluorination process. It is not surprising since elimination of certain oxygen-containing units have been often observed in the reactions between small organic compounds and DAST.[16]

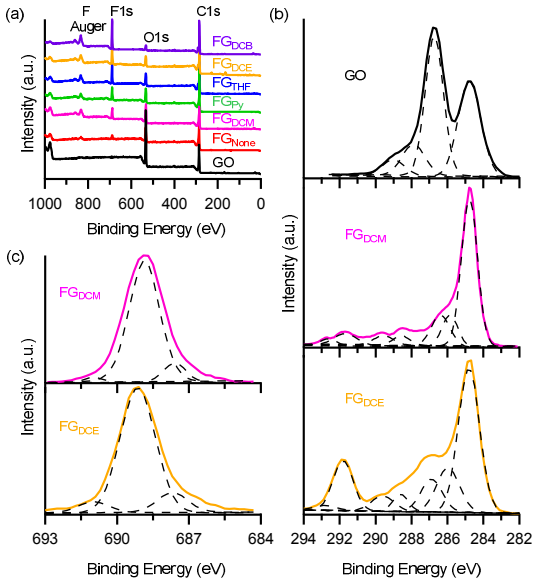

View Article Online
DOI: 10.1039/C4TA00847B

Fig. 1 (a) Survey XPS spectra of GO and the fluorinated graphene products. (b) C1s XPS spectra of GO, FG_{DCM} and FG_{THF}. (c) F1s XPS spectra FG_{DCM} and FG_{DCE}.

The detailed information of functionality transformation during the reaction was disclosed by X–ray photoelectron spectroscopy (XPS). In the XPS spectrum of GO (Fig. 1a), only two peaks around 286 and 533 eV, assignable to C 1s and O 1s core level peak respectively, were observed. The deconvolution of this C 1s peak yielded four components centred at 284.8, 286.5, 287.8 and 289.0 eV (Fig. 1b), associating with C–C/C=C, C–O, C=O, and COOH moieties, respectively.[17] In comparison, all the fluorinated graphene products displayed two additional peaks at 688.8 and 833.8 eV. These peaks originate photoemission from the F 1s core level and Auger electron, respectively, of CF, CF_2 and CF_3 units.[18] Moreover, in the C 1s peaks of all fluorinated graphene samples (Fig. 1b, and Fig. S1c, ESI†), new components around 285.9, 286.7, 288.5, 289.7, 291.6 and 292.9 eV were obtained after deconvolution and could be attributed to C–CF, C–CF_2, CF, CF–CF_2, CF_2 and CF_3 moieties, respectively.[3a, 19] The presence of CF, CF_2 and CF_3 units was further confirmed by the F 1s core level components located around 687, 689 and 691 eV, respectively (Fig. 1c and insets of Fig. S1c, ESI†). All these observations indicate that the oxygen-containing functionalities were successfully transformed into fluorinated units. In fact, according to fluoroorganic chemistry, when DAST meets with hydroxyl unit, a F anion-mediated nucleophilic substitution reaction will happen and convert the hydroxyl into CF unit.[16] Besides, DAST can react with carbonyl and carboxylic units via addition and nucleophilic substitution mechanisms and convert them into CF_2 and CF_3, respectively.[16] Furthermore, the variation of the XPS peak intensity also reflects the chemical change during the reaction. For example, the C–O component in C 1s core level peak of GO was very intense. However, it decreased after fluorination with DAST. This change, together with the decrease in the intensity of O 1s core level peak around 533 eV, implies the elimination of certain oxygen-containing units during the reaction. In addition, the change of F 1s core level peak intensity among the fluorinated graphene products suggests the fluorine-loading amount follows the order of $FG_{None} < FG_{DCM} < FG_{Py} < FG_{THF} < FG_{DCE} < FG_{DCB}$, which is coinciding well with the elemental analysis.

To further investigate bonding types of fluorinated units, solid-state ^{19}F NMR was performed on all fluorinated graphene products.[20] As shown in Fig. 2a, all the fluorinated graphene products displayed three distinguished signals at -56, -122, and -188 ppm in their solid-state ^{19}F NMR spectra. These signals originate from CF_3, CF_2, and C(sp^3)–F bonds, respectively. Besides these peaks, FG_{None} and FG_{Py} exhibited a new peak at -151 ppm, probably attributed to C(sp^2)–F bond. Meanwhile, an additional CF_3 peak at -76 ppm appeared in the solid-state ^{19}F NMR spectrum of FG_{THF}. These results agree well with XPS analysis.

The formation of C–F covalent bonds was also confirmed by the Fourier transform infrared spectroscopy (FT-IR). In FT-IR (Fig. 2b), GO presented strong peaks centred at 3340, 1732, 1223 and 1055 cm^{-1}, which can be assignable to the vibrations of O–H, C=O, C–OH and epoxy C–O functional groups, respectively.[21] After fluorination, a strong new band at 1215 cm^{-1}, the characteristic vibration modes of C–F, emerged.[4, 6b]

Raman spectroscopy was also used to characterize GO and fluorinated graphene products (Fig. S2, ESI†). All the spectra displayed two typical Raman resonances at 1590 and 1350 cm^{-1}. The former peak is G band of carbon materials, originating from in-plane bond stretching of sp^2 carbons. The latter is D band, caused by disordered sp^3 carbon bonding. Their intensity ratio (I_D/I_G) is well associated with the size of in-plane crystal domains, and thus is often employed to evaluate the disorder extent in graphitic structures. In this study, the I_D/I_G ratio of GO was estimated to be 1.98. After treatment with DAST, it changed to 1.42 for FG_{DCM}, 1.66 for FG_{DCE}, and 1.25 for FG_{None}. The decreased I_D/I_G value supports the loss of oxygen functionalities and the restore of the aromatic structure during fluorination process.

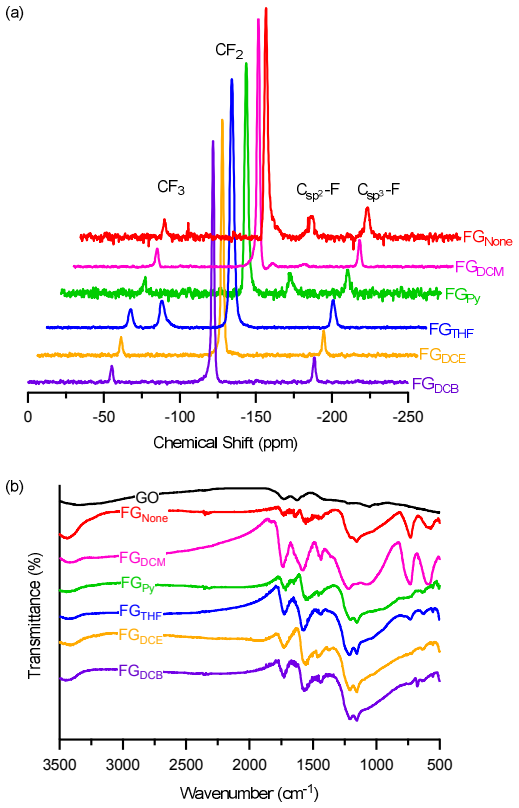

Fig. 2 (a) Solid-state ^{19}F NMR spectra of fluorinated graphene products. (b) FT-IR spectra of GO and fluorinated graphene products.

The morphology and microstructure of fluorinated graphene sheets were observed by field-emission scanning electron microscopy (FE-SEM), transmission electron microscopy (TEM) and atomic force microscopy (AFM) techniques. As shown in Fig. 3a–b, and S3 (ESI†), all freeze-dried fluorinated graphene products appeared like crumpled papers in their FE-SEM images. TEM further revealed that the fluorinated graphene sheets are transparent and flexible with wrinkled and

ARTICLE View Article Online DOI: 10.1039/C4TA00847B Journal Name

folded edges, resembling soft silk veils (Fig. 3c–d, and S4, ESI†). Normal-incidence selected area electron diffraction (SAED) analysis revealed that FG_{None}, FG_{DCM} and FG_{Py} have high crystal quality with the appearance of well-defined six-fold-symmetry pattern. In contrast, the SAED patterns of FG_{THF}, FG_{DCE} and FG_{DCB} showed annular diffraction pattern, suggesting polycrystals for their structures. The thickness of single-layer fluorinated flakes was estimated by AFM to be around 2.0 nm (Fig. 3e–f, and S5, ESI†), larger than that of GO. This means that the fluorinated carbon nanosheets are not one-atom thin layer structure like graphene. Some fluorinated moieties may stand outside the central layer and make the flake thicker.

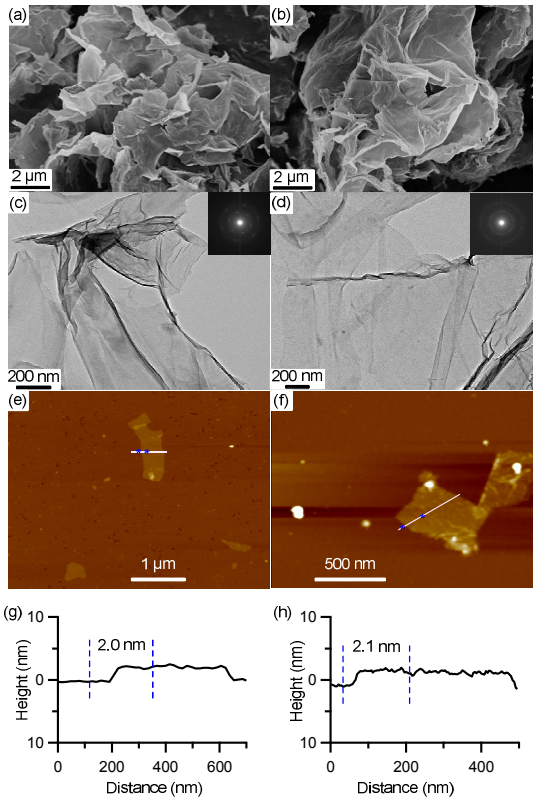

Fig. 3 FE-SEM (a, b), TEM (c, d), AFM (e, f) images and corresponding height profiles (g, h) of FG_{DCM} (a, c, e, g) and FG_{DCE} (b, d, f, h). Insets of (b) and (c) show their SAED pattern.

To understand the optical properties and electronic structure of the fluorinated graphene products, UV-vis and photolumiescent spectroscopies were applied as probes. The recorded spectra of all the samples dispersed in CH_3CN are displayed in Fig. 4 and their data are summarized in Table 2. It is obvious that all the fluorinated graphene samples exhibited a typical absorption peak around 220 nm (Fig. 4a). This peak is probably related to π-π* transition for the conjugated polyene-type structures in the carbon nanosheets.[22] In addition to this peak, at least one other peak appeared in the range of 250-350 nm in their absorption spectra for all fluorinated graphene products, suggesting the presence of a couple of conjugated aromatic domains with different sizes.[23] The longest absorption peak may be attributed to π-π* transition band from the largest aromatic domain. Its onset wavelength ($\lambda_{abs,\ onset}$) may represent the narrowest bandgap of the materials. Under this hypothesis, the bandgap of FG_{None} with 3.6% fluorine loading was estimated to be 2.73 eV, while that for FG_{DCM}, FG_{Py}, FG_{THF}, and FG_{DCE} are 2.85, 2.97, 3.65, and 3.58 eV respectively. The largest bandgap was found to be 3.79 eV, which is for FG_{DCB}, the product with largest fluorine loading (23.1%) among the family. This bandgap is larger than that of GO, which is estimated to be 3.46 eV (Fig. S6, ESI†). It is clear and reasonable to observe that the material bandgap increases upon the increment of fluorine loading amount and finally exceeds that of GO. In the photo-luminescent spectroscopy (Fig. 4b), all fluorinated graphene samples displayed photoluminescence upon excitation at 265 nm. Moreover, a couple of emission peaks with different positions were observed, coinciding with the multiple absorption bands in the UV-vis absorption spectroscopy. These results suggest the obtained carbon nanosheets may possess a number of conjugated aromatic domains with different sizes.[23]

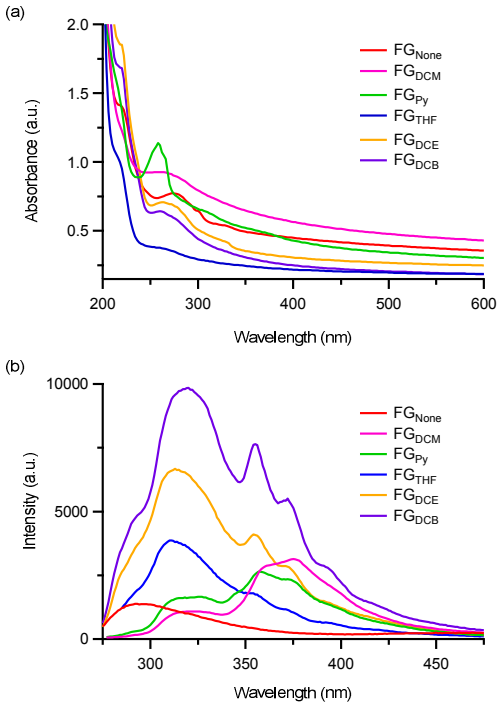

Fig. 4 (a) UV-vis absorption and (b) photo-luminescent spectra of fluorinated graphene samples in CH_3CN solution with a concentration of 2.5×10^{-3} mg/mL. The excitation wavelengths for all photo-luminescent spectra were 265 nm.

View Article Online
DOI: 10.1039/C4TA00847B

Table 2 Optical properties of fluorinated graphene samples in CH_3CN solution

Sample	$\lambda_{Abs,\ max}$ (nm)	$\lambda_{Abs,\ onset}$ (nm)	E_g [a] (eV)	$\lambda_{emission}$ (nm)
FG_{None}	220, 279, 301, 333	454	2.73	293
FG_{DCM}	219, 270	435	2.85	316, 360, 376
FG_{Py}	219, 258, 266, 312	417	2.97	314, 356, 373
FG_{THF}	218, 267	340	3.65	311, 354, 372
FG_{DCE}	220, 274, 331	346	3.58	314, 355, 372
FG_{DCB}	220, 262, 278	327	3.79	320, 355, 373

[a] Calculated by $1240/\lambda_{Abs,\ onset}$

The so-prepared fluorinated graphene products can be well and stably dispersed in varieties of organic solvents, including ethanol, THF, CH_3CN, chloroform, DMF, DMSO, and NMP, but not in water (Fig.S7, ESI†). By simply vacuum filtration from their CH_3CN dispersions, free-standing films were successfully prepared (Fig. 5a, inset). The films were flexible and strong enough for electrical conductivity measurement via a four-probe method. The result revealed that the electrical conductivity decreases when the fluorine content increases in the samples (Fig. 5a). For example, FG_{None} showed an electrical conductivity of 852.6 S m^{-1}, while that for FG_{DCB} was only as low as 0.091 S m^{-1}. Undoubtedly, more fluorine loading would decrease the content of conjugated aromatic structures, and thus not favourable for electrical conduction.

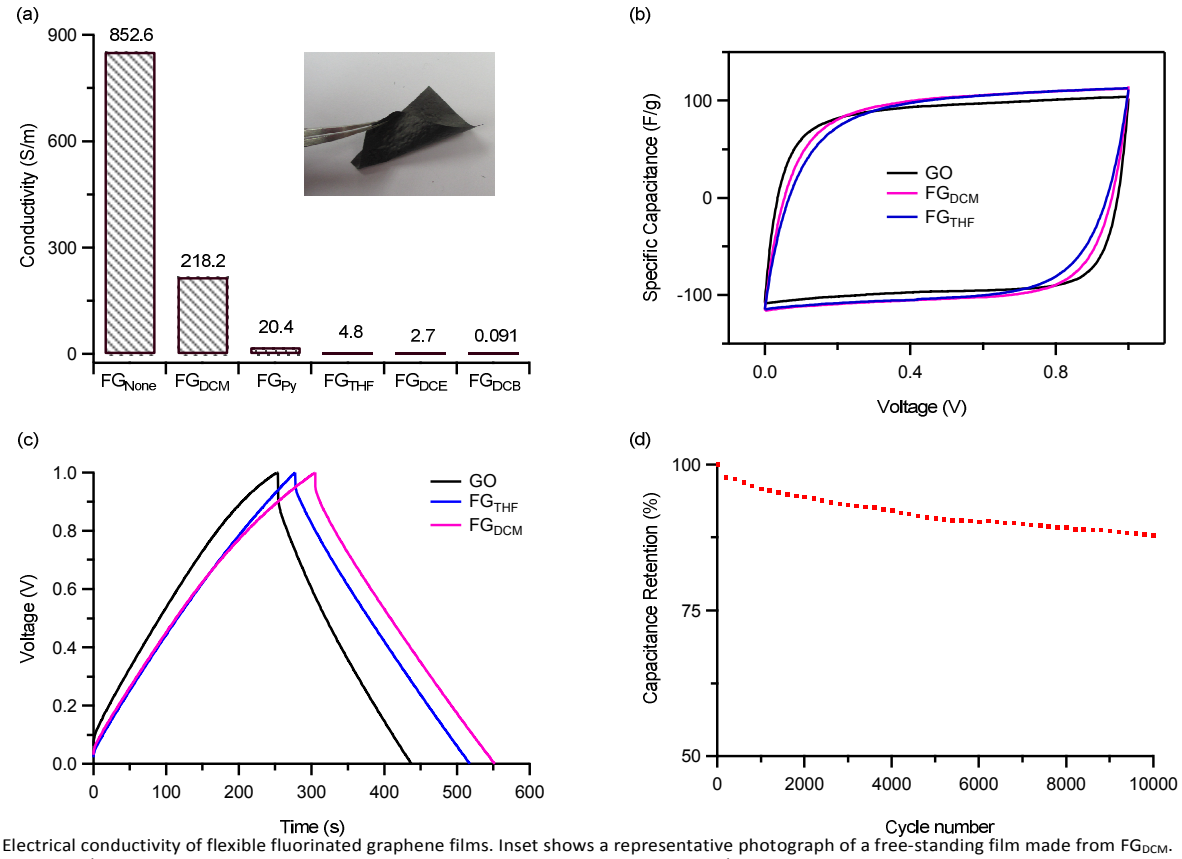

Fig. 5 (a) Electrical conductivity of flexible fluorinated graphene films. Inset shows a representative photograph of a free-standing film made from FG_{DCM}. (b) CV scanning at 10 mV s^{-1} and (c) galvanostatic charge/discharge curves at a current density of 0.5 A g^{-1} for the solid-state supercapacitor devices based on FG_{DCM}, FG_{THF} and GO. (d) Stability of FG_{DCM}-based device upon charge/discharge cycling at a current density of 0.1 A g^{-1}.

To evaluate the potential application of the so-prepared fluorinated graphene as electrode material for solid-state supercapacitors, we chose FG_{DCM} and FG_{THF} with different F-loading amounts as representatives together with GO to fabricate solid-state supercapacitors, and performed cyclic voltammetry (CV) and chronopotentiometry in a voltage range from 0 to 1.0 V. Here, Na_2SO_4-based hydrogel films were selected as electrolytes for solid-state supercapacitors for the advantages of no-leakage, an easy preparation process, and convenience in cell assemble, as compared to liquid based electrolytes. In CV measurements at a scan rate of 10 mV s^{-1} (Fig. 5b), all these devices displayed a nearly rectangular loop, indicating an excellent capacitive behaviour. From these loops, the specific capacitance was estimated to 106.6, 94.4 and 81.3 F g^{-1} for the devices based on FG_{DCM}, FG_{THF} and GO, respectively. Moreover, the charge/discharge curves (Fig. 5c) at a current density of 0.5 A g^{-1} show good symmetry and nearly linear slopes, which is another indicative of efficient electrical double layer (EDL) formation. From the discharge curves, the specific capacitance of FG_{DCM}, FG_{THF} and GO was calculated to be 104.8, 99.6, and 80.1 F g^{-1}, respectively. Apparently, the fluorinated graphene had better energy storage

ARTICLE View Article Online DOI: 10.1039/C4TA00847B Journal Name

properties than GO. However, the two fluorinated graphene materials having quite different fluorine-loading amount (6.0% for FG_{DCM}, 16.2% for FG_{THF}) displayed comparable performance. Compared with the reported graphene-based EDL solid-state supercapacitors,[24] the performance of our devices is moderate in the field. However, N_2 absorption and desorption experiments and Brunauer-Emmett-Teller (BET) analyses (Fig. S8, ESI†) disclosed that both FG_{DCM} and FG_{THF} have a very small specific surface area (9.8 and 11.3 m^2 g^{-1}, respectively). Therefore, there is much room to improve the energy storage performance of so-prepared fluorinated graphene as electrode materials for supercapacitors. Finally, we tested the cycling stability of the device based on FG_{DCM} and found that 88% of the original specific capacitance can be kept after 10000 charge/discharge cycles at a current density of 0.1 A g^{-1} (Fig. 5d).

Conclusions

In summary, we have demonstrated here a novel and facile solution method for fluorinated graphene preparation using GO as a starting material. Upon treatment with DAST, the oxygen-containing functionalities in GO can be easily transformed into fluorinated moieties, resulting in conversion of GO into fluorinated graphene. The detailed structural characterization confirms the presence of at least three types of fluorinated units, including CF, CF_2 and CF_3, in the product. Moreover, just by simply altering the reaction solvent, the fluorine-loading amount can be well tuned, and thus allow to tailor the optical and electronic properties of the final product. Since GO can be massively prepared from natural graphite in low cost and DAST is a commercially available liquid agent, the present approach may be suitable for large scale production of fluorinated graphene materials. Besides the preliminary studies showed that fluorinated graphene materials have potential use as electrode materials for energy storage, its real application in a wide range area would be a subject worthy further investigation.

Experimental section

Materials

Preparation of graphene oxide (GO). GO was synthesized from graphite flakes by utilizing a modified Hummers' procedure.[15] The natural graphite flakes (5.0 g, Alfa Aesar, 325 mesh) were added to a mixture of H_2SO_4 (120 ml, 98%) and $NaNO_3$ (2.5 g), and left stirring under ice-water bath for 1 h. Then, $KMnO_4$ (15.0 g) was added into the above mixture in portions within 30 min. After the reaction mixture was stirred at 20 ºC for 2 h, and then at 35 ºC for 30 min, deionized water (250 mL) was added carefully within 10 min and followed by additional stirring for 15 min. Eventually, a golden paste was produced by adding the mixture of deionized water (500 mL) and H_2O_2 aqueous solution (50 mL, 30%). The produced GO was collected by filtration, then subjected to thoroughly wash with HCl aqueous solution (500 mL, 5%) and deionized water (5000 mL), and finally freeze-dried, giving a yield of 4.6 g. AFM confirmed that the most of GO sheets stay single-layered with topographic height of around 1.0 nm (Fig. S5, ESI†). Elemental analysis found (%): C 51.5, H 3.4, N 1.2.

Preparation of fluorinated graphene (FG). Fluorinated graphene was prepared by mild liquid-phase reaction between GO and DAST. In a typical procedure, freshly distilled solvent (150 ml) and GO powder (0.15 g) was sequentially added into a 250 ml PTFE flask. The mixture was vigorously stirred overnight to promote GO dispersing. Afterwards, DAST (2.5 ml) was added dropwise at 0 ºC within 10 min. The reaction mixture was first treated with ultrasonication for 6 h, and then stirred for 3 d at ambient conditions. Finally, the reaction was quenched by carefully adding 100 ml methanol. The fluorinated products were obtained by filtration of the mixture over a 0.22 μm PTFE membrane, and subsequently subjected to thorough wash with ethanol, acetone, chloroform, THF and deionized water to remove impurities and dried in vacuum at 60 °C for 12 h.

FG_{None}. GO (0.150 g) was reacted with DAST (7.5 ml) without adding solvent, affording 0.128 g FG_{None}. Elemental analysis found (%): C 62.8, H 3.1, N 1.1, F 3.6.

FG_{DCM}. GO (0.150 g) was reacted with DAST (2.5 ml) in dichloromethane (DCM), affording 0.133 g FG_{DCM}. Elemental analysis found (%): C 64.3, H 2.1, N 0.9, F 6.0.

FG_{Py}. GO (0.150 g) was reacted with DAST (2.5 ml) in pyridine (Py), affording 0.135 g FG_{Py}. Elemental analysis found (%): C 58.8, H 2.8, N 1.4, F 8.7.

FG_{THF}. GO (0.150 g) was reacted with DAST (2.5 ml) in tetrahydrofuran (THF), affording 0.142 g FG_{THF}. Elemental analysis found (%): C 65.6, H 3.2, N 1.0, F 16.2.

FG_{DCE}. GO (0.150 g) was reacted with DAST (2.5 ml) in 1,2-dichloroethane (DCE), affording 0.147 g FG_{DCE}. Elemental analysis found (%): C 64.5, H 2.4, N 0.7, F 17.5.

FG_{DCB}. GO (0.150 g) was reacted with DAST (2.5 ml) in *o*-dichlorobenzene (DCB), affording 0.152 g FG_{DCB}. Elemental analysis found (%): C 59.8, H 1.7, N 0.6, F 23.1.

Fabrication and characterization of solid-state supercapacitors

Solid-state supercapcitors electrodes were prepared from fluorinated graphene powders blended with a polytetrafluoroethene aqueous suspension (PTFE, 60 wt%) and acetylene black. Fluorinated graphene was used as the active material for the adsorption and diffusion of electroactive species. PTFE and acetylene black were acted as a binder and conductor, respectively. The mass ratio of the active material, PTFE and acetylene black was 8:1:1. The slurry was pasted onto a stainless steel collector. Finally, the fluorinated graphene electrodes with a mass loading of about 1 mg cm^{-2} were dried in vacuum at 120 °C for 24 h.

Hydrogel electrolytes were prepared through photopolymerization of methyl methacrylate (MMA) with *N*,*N*'-methylenebisacrylamide as a cross-linker and 2,2-diethoxyacetophenone as a photo-initiator in the presence of Na_2SO_4 under UV irradiation. In a typical experiment, a

View Article Online
DOI: 10.1039/C4TA00847B

Maxima ML-3500C lamp (Spectronics Corp, USA), which can provide an intensity of 20.4 mw/cm^2 at 365 nm, was used as UV light source. A mixture of Na_2SO_4 (87.8 wt%, 0.6 M), MMA (10 wt%), *N*,*N*'-methylenebisacrylamide (2 wt%), and 2,2-diethoxyacetophenone (0.2 wt%) was subjected to UV irradiation for 20 min, affording a hydrogel electrolyte that can be adhered to the surface of fluorinated graphene electrodes as an integrated electrolyte and separator.

The supercapacitors were assembled in a symmetrical two-electrode sandwich configuration, namely, a test cell consisting of one hydrogel electrolyte film and two fluorinated graphene electrodes. The thickness of the hydrogel electrolyte layer was 100 μm. The performance characteristics of the supercapacitor cells were evaluated using cyclic voltammetry and chronopotentiometry. The gravimetric specific capacitance, C_{sp} (F g^{-1}), for a single electrode was calculated according to

$$C_{sp} = \frac{4I}{m\, dV/dt}$$

where I is the constant current, m is the total mass of the active material for both electrodes, and dV/dt was calculated from the slope obtained by fitting a straight line to the discharge curve over the range of V_{max} to (1/2)V_{max}.

Materials Characterization

Elemental analysis on carbon, hydrogen and nitrogen contents was carried out with an Elementar vario EL III elemental analyzer. The content of fluorine element was measured by a typical oxygen flask combustion method, in which the sample was burned in an oxygen atmosphere, and the produced inorganic fluorine ion was collected and titrated with thorium nitrate. Solid state ^{19}F NMR was recorded on a Bruker AVANCE III 376 M spectrometer. Fourier transform infrared (FT-IR) spectra were recorded on a Nicolet Avatar-360 Fourier transform infrared spectrophotometer using a KBr pellet. Raman spectra were measured on a Renishaw inVia Reflex micro-Raman spectrometer using a 100-fold objective lens and a crystal laser excitation at 514.5 nm with a power of 0.1 mW. The morphology of fluorinated graphene samples was investigated by a Hitachi S-4800 field emission scanning electron microscope (FE SEM) operating at 3 kV. Samples were prepared by freeze-dried and immobilized on a conductive tape. Transmission electron microscopy (TEM) and selected area electron diffraction (SAED) were performed on a JEOL JEM-2010 microscope operating at 120 kV. Samples were prepared by placing a drop of very dilute acetonitrile dispersion on a holey-carbon-coated copper grid and dried at ambient conditions. Atomic force microscopy (AFM) was performed under ambient conditions on a Veeco instrument Nanoscope IIIa Multimode apparatus operating in a non-contact mode with a silicon tip and cantilever operating at a frequency of 325 kHz and a scanning speed of 0.2 Hz. Samples were prepared by placing a drop of very dilute acetonitrile dispersion on a silicon substrate and dried in vacuum at room temperature. X-ray photoelectron spectroscopy (XPS) was recorded on a PHI-5000 VersaProbe spectrometer under 10^{-7} Pa using monochromatic Al K_α X-ray source operating at 100 W. The sheet resistance (R_s) of fluorinated graphene papers prepared by filtering their acetonitrile dispersions was measured by a means of a four-point probe method on a SX-1944 digital instrument. The conductivity was calculated based on sheet resistance and the thickness of the film. UV-vis absorption and fluorescence spectroscopies were performed on a Hitachi U-3310 spectrophotometer and a Hitachi F4600 spectrofluorometer, respectively, at room temperature. The N_2 adsorption and desorption isotherms were measured at 77 K on an automatic adsorption instrument (Micromeritics TriStar 3000). Prior to the gas sorption measurements, all the samples were vacuumed at 120 °C for 24 h. The specific surface area was calculated using the Braunauer-Emmett-Teller (BET) method, and the relative pressure range of P/P$_0$ from 0.1 to 0.3 was used for multipoint BET calculations.

Acknowledgements

We gratefully acknowledge the financial support from National Natural Science Foundation of China (No. 21074147), National Basic Research Program of China (2012CBA01200), Shanghai Science and Technology Commission (No. 13JC1407000), and Chinese Academy of Sciences.

Notes and references

[a] Laboratory of Synthetic and Self-Assembly Chemistry for Organic Functional Molecules, Shanghai Institute of Organic Chemistry, Chinese Academy of Sciences, 345 Lingling Road, Shanghai 200032, China. E-mail: liws@mail.sioc.ac.cn.

[b] Key Laboratory of Organofluorine Chemistry, Shanghai Institute of Organic Chemistry, Chinese Academy of Sciences, 345 Lingling Road, Shanghai 200032, China. E-mail: chenqy@mail.sioc.ac.cn.

[c] Department of Chemistry, Tongji University, 1239 Siping Road, Shanghai 200092, China. E-mail: wangqg66@tongji.edu.cn.

† Electronic Supplementary Information (ESI) available: XPS, Raman, FE-SEM, TEM, AFM, dispersibility, and BET characterization of fluorinated graphene. See DOI: 10.1039/b000000x/

‡ These authors contributed equally to this work

1 F. Karlicky, K. K. R. Datta, M. Otyepka and R. Zboril, *ACS Nano*, 2013, **7**, 6434.

2 R. Nair, W. Ren, R. Jalil, I. Riaz, V. G. Kravets, L. Britnell, P. Blake, F. Schedin, A. S. Mayorov, S. Yuan, M. I. Katsnelson, H.-M. Cheng, W. Strupinski, L. G. Bulusheva, A. V. Okotrub, I. V. Grigorieva, A. N. Grigorenko, K .S. Novoselov and A. K. Geim, *Small*, 2010, **6**, 2877.

3 a) J. T. Robinson, J. S. Burgess, C. E. Junkermeier, S. C. Badescu, T. L. Reinecke, F. K. Perkins, M. K. Zalalutdniov, J. W. Baldwin, J. C. Culbertson, P. E. Sheehan and E. S. Snow, *Nano Lett*., 2010, **10**, 3001; b) K. J. Jeon, Z. Lee, E. Pollak, L. Moreschini, A. Bostwick, C.-M. Park, R. Mendelsberg, V. Radmilovic, R. Kostecki, T. J. Richardson and E. Rotenberg, *ACS Nano*, 2011, **5**, 1042.

ARTICLE View Article Online DOI: 10.1039/C4TA00847B Journal Name

4 Y. Wang, W. C. Lee, K. K. Manga, P. K. Ang, J. Lu, Y. P. Liu, C. T. Lim and K. P. Loh, *Adv. Mater*., 2012, **24**, 4285.

5 R. Romero-Aburto, T. N. Narayanan, Y. Nagaoka, T. Hasumura, T. M. Mitcham, T. Fukuda, P. J. Cox, R. R. Bouchard, T. Maekawa, D. S. Kumar, S. V. Torti, S. A. Mani and P. M. Ajayan, *Adv. Mater*., 2013, **25**, 5632.

6 a) H. Chang, J. Cheng, X. Liu, J. Gao, M. Li, J. Li, F. Tao, F. Ding and Z. Zheng, *Chem. Eur. J.,* 2011, **17**, 8896; b) M. Zhang, Y. Ma, Y. Zhu, J. Che and Y. Xiao, *Carbon*, 2013, **50**, 149.

7 W.-K. Lee, J. T. Robinson, D. Gunlycke, R. R. Stine, C. R. Tamanaha, W. P. King and P. E. Sheehan, *Nano Lett*., 2011, **11**, 5461.

8 K. Tahara, T. Iwasaki, A. Matsutani and M. Hatano, *Appl. Phys. Lett*., 2012, **101**, 163105.

9 H. Yang, M. Chen, H. Zhou, C. Qiu, L. Hu, F. Yu, W. Chu, S. Sun and L. Sun, *J. Phys. Chem. C*, 2011, **115**, 16844.

10 X. Yu, K. Lin, K. Qiu, H. Cai, X. Li, J. Liu, N. Pan, S. Fu, Y. Luo and X. Wang, *Carbon*, 2012, **50**, 4512.

11 W. H. Lee, J. W. Suk, H. Chou, J. Lee, Y. Hao, Y. Wu, R. Piner, D. Akinwande, K. S. Kim and R. S. Ruoff, *Nano Lett*., 2012, **12**, 2374.

12 a) D. Chen, H. Feng and J. Li. *Chem. Rev.*, 2012, **112**, 6027; b) V. Georgakilas, M. Otyepka, A. B. Bourlinos, V. Chandra, N. Kim, K. C. Kemp, P. Hobza, R. Zboril and K. S. Kim, *Chem. Rev.*, 2012, **112**, 6156.

13 Z. Wang, J. Wang, Z. Li, P. Gong, X. Liu, L. Zhang, J. Ren, H. Wang and S. Yang, *Carbon*, 2012, **50**, 5403.

14 X. Wang, Y. Dai, J. Gao, J. Huang, B. Li, C. Fan, J. Yang and X. Liu, *ACS Appl. Mater. Interfaces*, 2013, **5**, 8294.

15 F.-G. Zhao and W.-S. Li, *J. Mater. Chem*., 2012, **22**, 3082.

16 P. Kirsch, *Modern Fluoroorganic Chemistry: Synthesis, Reactivity, Applications*, WILEY-VCH, Weinheim, 2004.

17 Y. Xu, L. Zhao, H. Bai, W. Hong, C. Li and G. Shi, *J. Am. Chem. Soc.*, 2009, **131**, 13490.

18 P. Gong, Z. Wang, J. Wang, H. Wang, Z. Li, Z. Fan, Y. Xu, X. Han and S. Yang. *J. Mater. Chem*., 2012, **22**, 16950.

19 J.-M. Lee, S. J. Kim, J. W. Kim, P. H. Kang, Y. C. Nho and Y.-S. Lee, *J. Ind. Eng. Chem*., 2009, **15**, 66.

20 P. Meduri, H. Chen, J. Xiao, J. J. Martinez, T. Carlson, J.-G. Zhang and Z. D. Deng, *J. Mater. Chem. A* 2013, **1**, 7866.

21 J. R. Lomeda, C. D. Doyle, D. V. Kosynkin, W.-F. Hwang and J. M. Tour, *J. Am. Chem. Soc.*, 2008, **130**, 16201.

22 W. Zhang, J. Cui, C.-A. Tao, Y. Wu, Z. Li, L. Ma, Y. Wen and G. Li, *Angew. Chem. Int. Ed*., 2009, **48**, 5864.

23 P. Gong, J. Wang, W. Sun, D. Wu, Z. Wang, Z. Fan, H. Wang, X. Han and S. Yang, *Nanoscale* 2014, **6**, 3316.

24 (a) Y. Xu, Z. Lin, X. Huang, Y. Liu, Y. Huang and X. Duan, *ACS Nano* 2013, **7**, 4042. (b) C. J. Shearer, A. Cherevan and D. Eder, *Adv. Mater.* 2014, DOI: 10.1002/adma.201305254.

